

**Book of Tutorials and Abstracts**

---



European Microbeam Analysis Society

---

## **EMAS 2019**

**16th  
EUROPEAN WORKSHOP**

**on**

# **MODERN DEVELOPMENTS AND APPLICATIONS IN MICROBEAM ANALYSIS**

19 to 23 May 2019  
at the  
NTNU, Realfagbygget  
Trondheim, Norway

---

Organised in collaboration with:  
Norwegian University of Science and Technology  
(NTNU)

---



## **NANODIAMONDS FROM EARTH TO THE COSMOS**

Rhonda M. Stroud and B. De Gregorio

US Naval Research Laboratory, Materials Science and Technology Division  
4555 Overlook Avenue SW, 20375 Washington, DC, U.S.A.  
e-mail: rhonda.stroud@nrl.navy.mil

Rhonda Stroud is the Head of the Nanoscale Materials Section at the U.S. Naval Research Lab, where she oversees the US Defense Department's most advanced electron microscope facility for nanoscale materials characterisation, including a Nion UltraSTEM 200-X for single-atom sensitivity imaging and spectroscopy. Her research interests span many classes of materials, from quasicrystals and oxide electronics to aerogel nanocomposites and nanoparticles formed in supernovae. She received her B.A. in physics from Cornell University in 1991, and her PhD in physics from Washington University in St. Louis in 1996. She is a fellow of both the American Physical Society and the Meteoritical Society, and has an asteroid named in her honour by the International Astronomical Union. She is President of the Microanalysis Society of America, and serves on the NASA Planetary Science Division Advisory Committee.

Nanodiamonds are of broad scientific and technological interest. Industrially they find use as polishing compounds, wear-resistant coatings, and for drug delivery and bio-imaging. In future, they may also be employed in quantum computing applications, if more control can be achieved over incorporation of specific dopant atoms. At present, doping of synthetic nanodiamonds is accomplished by ion irradiation after the initial nanodiamond growth. However, this ion implantation introduces structural damage, and limits the type of dopants that can be incorporated. From a planetary science perspective, the incorporation of defects or impurity atoms into diamonds is also of particular interest, because specific impurity species offer clues to the cosmochemical provenance of the diamonds [1]. Primitive meteorites i.e., meteorites that made of materials minimally altered since the beginning of the solar system, contain nanodiamonds that in turn carry isotopically anomalous impurities indicative of formation by nucleosynthesis in supernovae. Because of the small size of the meteoritic nanodiamonds, only 2 nm on average, detection of the isotopically anomalous impurities has not yet been successful on an individual diamond basis. Instead, the meteoritic nanodiamonds are isolated from the host meteorites by acid treatments, and isotopic measurements are carried out on ensembles of millions or more particles at once. The abundance of these nucleosynthetic anomalies is very low, and it is not know which of the nanodiamonds formed at any given time or place in the galaxy. The most powerful tool for characterization of the incorporation of dopants into nanodiamonds, whether made in space or in the laboratory is an aberration-corrected scanning transmission electron microscope (STEM). With STEM, researchers can carry out imaging and spectroscopy studies at the single-atom scale, including spatially resolving  $sp^3$  (diamond) and  $sp^2$  (graphitic) bonding.

Although diamond is thermodynamically stable only at high temperature and pressure conditions, nanodiamonds can be produced as a metastable phase through multiple synthesis routes. Common methods include controlled detonation of organic precursors, physical abrasion / mechanical grinding of bulk diamond, chemical vapour deposition of thin films followed by acid dissolution of non-diamond components, and ion irradiation or laser ablation. Meteoritic nanodiamonds have been argued to form under natural versions of each of these processes, e.g., high-pressure / high-temperature (HP/HT) phase transformation induced by supernova shockwaves or grain-grain collisions, non-equilibrium condensation in stellar atmospheres, and UV irradiation of organic ices. Daulton *et al.* [2] argued on the basis of high-resolution TEM imaging of lattice twinning patterns that the meteoritic nanodiamonds appeared more similar to synthetic CVD nanodiamond (direct condensation under low pressure), than to detonation diamonds (HP/HT phase transformation). However, Daulton *et al.* [2] were not able to make a direct comparison of the twins in the 2 nm size regime, as the detonation nanodiamond were closer to 5 nm average diameter. Furthermore, noble gas release studies of meteoritic nanodiamonds isolates often show bi-modal release patterns, indicative of multiple sub-populations in the nanodiamond residues. Our prior work [3] revealed that these residues can contain up to 50 %  $sp^2$  carbon, and it is not yet know whether any the bimodal release patterns is associated with the presence of two phases of carbon, different subpopulation of diamonds, or simply different modes of incorporation into the diamond lattice.

In this study, we apply aberration-corrected STEM to the analysis of meteoritic nanodiamonds and synthetic nanodiamonds produced by HP/HT phase transformation [4]. Our goal is to provide proof-of-concept data for understanding how noble gases might get incorporated into nanodiamond in space environments, and to identify a pathway for future studies that could distinguish among nanodiamonds of solar system, interstellar or circumstellar origin. We examined nanodiamond samples with the Nion UltraSTEM 200-X at the Naval Research Lab, equipped with a Bruker Xflash 100 energy-dispersive X-ray (EDS) spectrometer, and Gatan Enfinitum HR electron energy loss spectrometer (EELS). The nanodiamond samples included: Microtome slices of in situ particles embedded in insoluble organic matter from the Murchison meteorite, acid-resistant residues from the Murchison and Allende meteorites, and doped nanodiamonds produced by high pressure / high temperature (HP/HT) phase transformation of carbon aerogels. The Nion was operated at 60 kV, with a nominal 0.15 nm, 50 - 100 pA probe. Heating stage experiments to observe the transformation of the Allende nanodiamond residues with temperature were carried out in the Nion using a Protochips Fusion system.

It has already been shown that the meteoritic nanodiamonds are associated with pockets of organic matter in the matrices of primitive meteorites [5]. Locating the nanodiamonds in situ in the organic matter is one way to derive additional contextual information for determination of the nanodiamond formation (Fig. 1). Although the nanodiamonds cannot be distinguished from the organic matter by high angle-annular dark field imaging alone, they can be readily identified through low loss EELS mapping, due to the diamond plasmon peak at 34 eV. Figure 1b shows an example 128 × 128 pixel map calculated from the difference in the low spectrum image intensity in 1 eV energy windows at 23 eV and 33.8 eV. The nanodiamonds appear as bright spots in low loss difference map. Our preliminary data indicates that the nanodiamonds are preferentially associated with the fine, fluffy organic matter, and not the dense organic matter that may have experienced more extensive processing on the asteroid parent of the host meteorite.

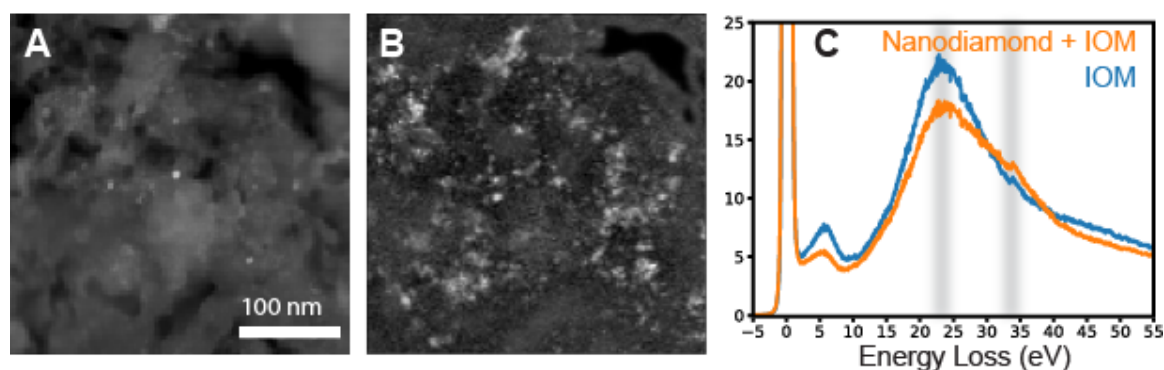


Figure 1. a) High-angle annular dark field, b) EELS two window difference map of nanodiamond distribution of in an insoluble organic matter isolate of the Murchison meteorite, and c) example low loss EEL sum spectra from the diamond-rich and diamond-poor regions of the spectrum image, showing the energy windows for difference map.

In order to analyse the meteoritic nanodiamonds at the single-atom scale, it is necessary to study them after further chemical processing to remove the surrounding organic matter. Figure 2 shows high-angle annular dark field images of nanodiamond isolates from the Murchison meteorite, and corresponding EDS data from a single diamond and nearby amorphous carbon. Bright white spots in these images correspond to individual atoms with  $Z > 6$ , including O, Si and S. Although N is present, the difference in atomic number between C and N is too small for the N impurities to be revealed by Z contrast. The EDS analyses suggest that certain impurities may be preferentially associated with either the nanodiamond (N, Si), or the amorphous carbon (O) components of the residues.

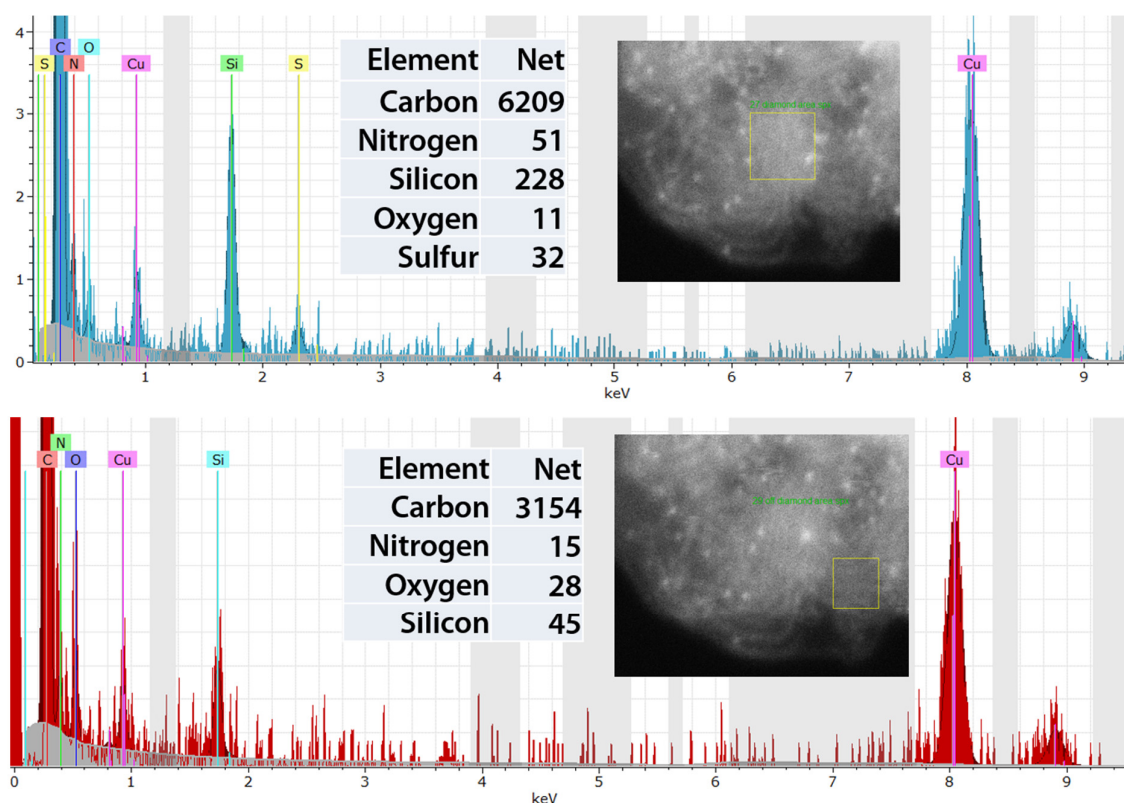


Figure 2. Top: Energy-dispersive X-ray spectrum from a single 4 nm nanodiamond (yellow box in inset). Bottom: Energy-dispersive X-ray spectrum from an amorphous carbon region of a nanodiamond residue (yellow box). The copper signal is from the sample grid and instrument. Comparison of the net counts from each samples area indicates that N is preferentially associated with the nanodiamond, and oxygen more associated with the amorphous carbon.

Meteoritic nanodiamond residues are often characterised by step-wise heating experiments, in which the gasses desorbed from the sample are elementally and isotopically characterised with mass spectrometry. Heating stage experiments in a UVH STEM can complement the mass spectrometry experiments, by identifying the temperature thresholds for physical changes to the

diamond, as tracked with dark field imaging, and C K-edge EELS measurements (Fig. 3). As a proof-of-concept measurement, we heated in situ in the Nion STEM an aliquot of an Allende nanodiamond residue, and tracked the sample changes with dark field imaging and electron energy loss spectroscopy (Fig. 3). The as-deposited sample shows the characteristic C K-edge EELS signature of diamond, along with a small  $\pi^*$ -peak at 284.3 eV, indicative of the  $sp^2$  component common to nanodiamonds. In addition, there is a small peak at  $\sim 282.4$  eV, reported to be associated with N impurities in diamond (N-V centres) [6], or with partially H-passivated surface defects [7]. In contrast, N defects in  $sp^2$  carbons, such as graphene, generate a low energy shoulder on the  $\sigma^*$ -peak [8], which is not observed here due to the low amount of  $sp^2$  carbon. In this Allende DM sample, which we measured to initially contain  $\sim 0.1$  to  $0.3$  at% N, the N defect peak dramatically decreases in intensity between  $400$  °C and  $600$  °C, well above the temperature at which surface H would be desorbed under the electron beam. This relatively low temperature release of N is important, because published stepped combustion studies show the lowest temperature N release to be the least isotopically anomalous, but definitive evidence that the low temperature N was carried by the diamond, rather than  $sp^2$  carbon or other components in the residues, was lacking. Our preliminary data show direct evidence that isotopically normal N measured in the residues is intrinsic to the diamond, and thus these diamonds are most likely Solar System in origin.

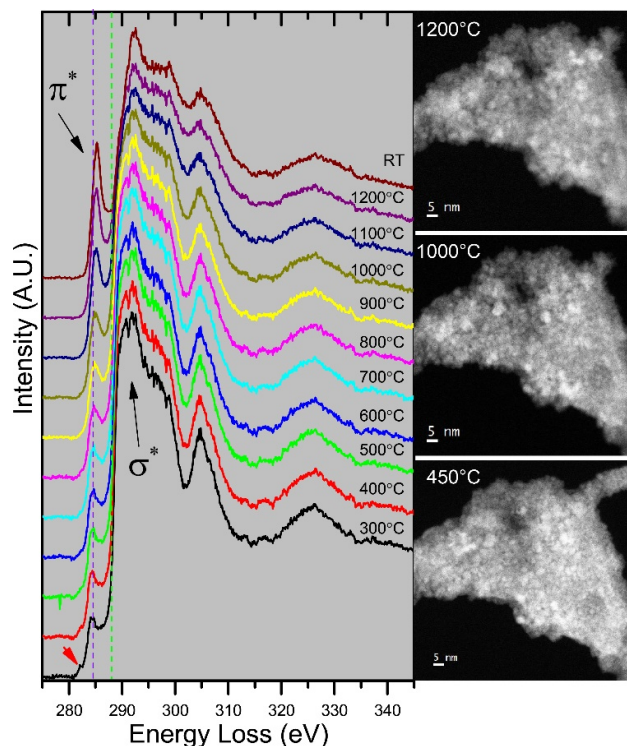


Figure 3. Carbon K-edge EELS and medium-angle annular dark field STEM image of Allende nanodiamond heated in situ in the UHV UltraSTEM. The red arrow at the bottom left indicates a peak associated with N defects in the diamond lattice. This peak is dramatically reduced in intensity by  $600$  °C due to the release of nitrogen from the diamonds. The increased contrast in the dark field image of the sample at  $1,000$  °C is due to the loss of impurities and surface carbon from the sample. By  $1,200$  °C, a significant fraction, but not all, of the sample has graphitized, as shown in the EELS data by the shift in the  $\pi^*$ -peak position and intensity, and the decrease in the “dip” at  $302$  eV.

Continued heating of the sample to 1,200 °C under UHV conditions causes a gradual increase in graphitisation, demonstrated by the relative intensity increase of the  $\pi^*$ -peak, a shift the centroid to 285.3 eV, and changes in the extended structure at higher energies, e.g., the decrease in the dip at 302 eV and increase in intensity between 295 eV and 300 eV. The most dramatic changes occur above 900 °C, including increased porosity, consistent with the onset of the release of HL components in pyrolysis experiments. By 1,200 °C the sample is at least 50 % graphitic C, and remains that way on cooling back to room temperature (Fig. 4).

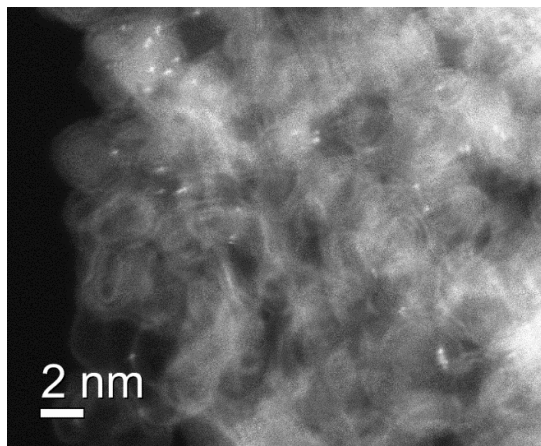


Figure 4. Dark field STEM image of the Allende DM sample heated to 1,200 °C and returned to room temperature in vacuum. Onion-like turbostratic layers of graphitic carbon are visible along with individual and clustered impurity atoms (white dots).

As a proof concept for the detection of impurities incorporated in into nanodiamond, we have also investigated nanodiamonds produced by HT/HP transformation of porous amorphous carbon aerogels. A combination of dark field imaging, EELS and EDS observations demonstrate that argon can be incorporated into HT/HP nanodiamond (Fig. 4) [3]. This suggests that one possible origin for nanodiamonds in the early solar system might have been collisional shock processing (HT/HP) of grains coated with organic ices rich in adsorbed noble gases.

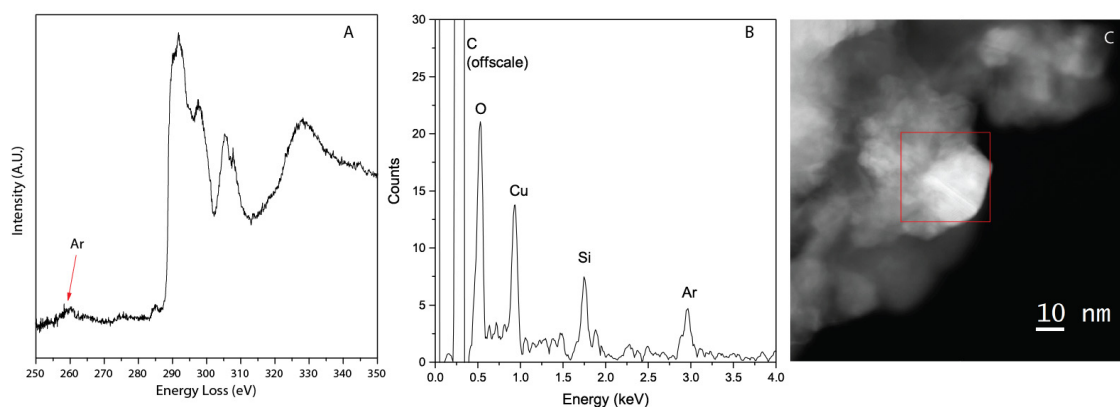


Figure 5. a) C K-edge EELS, and b) EDXS of the area outlined in red in (c); medium-angle annular dark field image of Ar-doped synthetic HT/HP nanodiamond.

In summary, aberration-corrected transmission electron microscopy imaging, electron energy loss spectroscopy and energy dispersive X-ray spectroscopy is an extremely powerful combination for tackling the very challenging problem of determining the possible origin(s) of meteoritic nanodiamonds. While it is generally agreed that the noble gas isotope studies of meteoritic nanodiamond residues demonstrate that some component of the residues has a signature of formation outside the solar system, it is not yet known what fraction of the nanodiamonds share this origin, or have distinct formation histories in the early solar system. The best chance at answering this question is through a series of coordinated experiments as outlined here: (1) identification of any special characteristics of organic matter that might be preferentially associated with the nanodiamond, by in situ mapping of the nanodiamonds with low loss EELS; (2) mapping of impurities in the diamond residues to search for preferential association of dopant and impurities atoms with either diamond or amorphous carbon phases; (3) hot stage experiments to track the morphological changes to the nanodiamonds under conditions that can be relate to noble gas release heating studies; and (4) comparison with noble-gas and N-doped synthetic nanodiamonds to better understand the range of doping conditions.

#### *ACKNOWLEDGEMENTS*

The authors gratefully acknowledge funding from the ONR/ NRL Core Program and NASA Emerging Worlds, and samples from: (Allende) J. Greer and P. Heck at the Field Museum in Chicago, IL, (synthetic) M. Crane and P. Pauzuskie at the University of Washington, and (Murchison) C.M. O'D. Alexander at the Carnegie Institution of Washington.

#### *6. REFERENCES*

- [ 1] Lewis R, *et al.* 1987 *Nature* **326** 162-164
- [ 2] Stroud R M, *et al.* 2011 *Astrophys. J. Lett.* **738**(2)
- [ 3] Daulton T, *et al.* 1996 *Geochim. Cosmochim. Acta* **60** 4853-4872
- [ 4] Crane M J, *et al.* 2018 *Diamond Rel. Mater.* **87** 134-142
- [ 5] Garvie L A J 2010 Where are the nanodiamonds in the primitive meteorites? Preliminary TEM results. in: *Proc. 2010 Lunar and Planetary Science Conference.* 1388
- [ 6] Chang H C, *et al.* 2016 Diamonds in space: a brief history and recent laboratory studies. in: *11th Pacific Rim Conf. on Stellar Astrophysics: Physics and Chemistry of the Late Stages of Stellar Evolution.* (Kwok S and Leung K C; Eds.) Pts 1-6
- [ 7] Garvie L A J 2006 *Meteoritics Planet. Sci.* **41** 667-672
- [ 8] Nicholls R J, *et al.* 2013 *ACS Nano* **7** 7145-7150